J. Membrane Biol. 171, 209–221 (1999)

The Journal of
Membrane
Biology

Diphtheria Toxin Forms Pores of Different Sizes Depending on Its Concentration in Membranes: Probable Relationship to Oligomerization

J.C. Sharpe, E. London

Department of Biochemistry and Cell Biology, Department of Chemistry, and the Institute for Cell and Developmental Biology, State University of New York at Stony Brook, Stony Brook, NY 11794-5215, USA

Received: 10 March 1999/Revised: 22 June 1999

Abstract. Diphtheria toxin forms pores in biological and model membranes upon exposure to low pH. These pores may play a critical role in the translocation of the A chain of the toxin into the cytoplasm. The effect of protein concentration on diphtheria toxin pore formation in model membrane systems was assayed by using a new fluorescence quenching method. In this method, the movement of Cascade Blue labeled dextrans of various sizes across membranes is detected by antibodies which quench Cascade Blue fluorescence. It was found that at low pH the toxin makes pores in phosphatidylcholine/phosphatidylglycerol vesicles with a size that depends on protein concentration. At the lowest toxin concentrations only the entrapped free fluorophore (MW 538) could be released from model membranes. At intermediate toxin concentrations, a 3 kD dextran could be released. At the highest toxin concentration, a 10 kD dextran could be released, but not a 70 kD dextran. Similar pore properties were found using vesicles lacking phosphatidylglycerol or containing 30% cholesterol. However, larger pores formed at lower protein concentrations in the presence of cholesterol. The dependence of pore size on toxin concentration suggests that toxin oligomerization regulates pore size. This behavior may explain some of the conflicting data on the size of the pores formed by diphtheria toxin. The formation of oligomers by membrane-inserted toxin is consistent with the results of chemical crosslinking and measurements of the self-quenching of rhodamine-labeled toxin. Based on these experiments we propose diphtheria toxin forms oligomers with a variable stoichiometry, and that pore size depends on the oligomerization state. Reasons why oligomerization could assist proper membrane insertion of the toxin and other proteins that convert from soluble to membrane-inserted states are discussed.

Key words: Fluorescence quenching — Model membranes — Membrane translocation

Introduction

Diphtheria toxin is a protein produced by *Corynebacterium diphtheriae.* The toxin is secreted as a single polypeptide (Mr 58,348), but can be readily cleaved by a furin-like protease into two subunits, A (Mr 21,167) and B (Mr 37,199), which are held together by a disulfide bond [15, 25]. The toxin has been shown to enter cells by receptor-mediated endocytosis. Once internalized, the acidification of the endosomal lumen triggers a pH-dependent conformational change that allows the toxin to penetrate the endosomal membrane [25]. After the disulfide bond that holds the A and B chains together is reduced, exposure to the neutral pH of the cytosol is believed to trigger the final step in translocation of the A chain across the bilayer and its release into the cytoplasm. Once released, the A chain catalyzes the ADP-ribosylation of elongation factor 2, inhibiting protein synthesis and causing cell death [11]. Elucidation of the mechanism of membrane penetration and translocation by diphtheria toxin is an important goal as it may have important implications for understanding: (i) viral fusion proteins that mediate viral penetration through acidic organelles, (ii) membrane insertion and translocation of newly synthesized membrane and secreted proteins, and (iii) the mechanism of apoptosis inhibition by the Bcl family of proteins, which appear to have a pore-forming domain similar to that of the toxin [35].

The crystal structure of the toxin has been solved in solution [8], but its structure in membranes has only

Correspondence to: E. London

begun to be characterized. As a result, the mechanism of A chain translocation across membranes is unknown, although several models have been proposed. One proposed mechanism involves pore formation. Many groups have demonstrated that the toxin can form a pore in model and cellular membranes [13, 20, 22–24, 30, 32, 36, 44]. Using mutant toxins it has been shown that the ability of the toxin to induce pore formation is correlated with its translocation and/or toxicity [14, 37]. However, it is not clear whether this means translocation requires a pore, or reflects a dependence of both pore formation and translocation on proper membrane insertion. Furthermore, it is not clear whether pore size is sufficient to allow A chain translocation directly through the pore (*see* Discussion).

In addition, evidence from a number of studies demonstrating A chain interaction with lipids has suggested a translocation mechanism that might not involve A chain passage through an aqueous pore formed by the B chain. For example, photolabeling studies and studies of the interaction of the isolated A chain with bilayers have demonstrated that the A chain inserts into the membrane and can come into direct contact with the acyl chains of the lipid bilayer [17, 31, 33, 44, 45]. In addition, we have recently obtained evidence that the T domain may function by a chaperone-like activity (J. Ren, K. Kachel, S. Malenbaum, R.J. Collier, and E. London, *unpublished observations*). Overall, there remains considerable uncertainty about the role of pores in translocation.

In this study, a new fluorescence-quenching technique has been used to investigate the size of the pores formed by diphtheria toxin in more detail. We find pore size clearly depends on the concentration of toxin in the membrane. This may explain some of the uncertainty about pore size from earlier studies, and suggests that toxin oligomerization controls pore size. In support of this proposal evidence indicating toxin oligomerization in membranes is presented. The results of this study lay a foundation for examining the role of pore formation in the translocation process.

Materials and Methods

Materials

Anti-Cascade Blue rabbit IgG (H+L fractions) antibody (Ab) (2.5–2.8 mg/ml stock solution), Cascade Blue (CB) labeled dextrans (molecular weight 3 kD, 10 kD, 70 kD), the free Cascade Blue dye, 8-methoxypyrenetrisulfonic acid (MPT; molecular weight 538 daltons), 10% lissamine rhodamine-B sulfonyl chloride (LRB-SO_2Cl) on celite, and N-(1-pyrenesulfonyl)-1,2-dihexadecanoyl-sn-glycero-3-phosphoethanolamine, triethylammonium salt (pyrene-PE) were purchased from Molecular Probes (Eugene, OR). The lipids N-(Lissamine rhodamine B sulfonyl)-1,2-dihexadecanoyl-sn-glycero-3-phosphoethanolamine, triethylammonium salt (rhodamine-PE), N-(7-nitro-2,1,3-benzoxadiazol-4-yl)-1,2-dihexadecanoyl-sn-glycero-3-phosphoethanolamine (NBD-PE), 1,2-dioleoyl-sn-glycero-3-phosphocholine (DOPC), and 1,2-dioleoyl-sn-glycero-3-[phospho-rac(1 glycerol)] (DOPG) were purchased from Avanti Polar Lipids (Alabaster, AL). Cholesterol and cytochrome C were purchased from Sigma. Disuccinimidyl propionate (DSP) and disuccinimidyl tartarate (DST) were purchased from Pierce Chemical. Partially purified diphtheria toxin was purchased from Connaught Laboratories (Ontario, Canada) and further purified as previously described [5, 28]. The toxin was stored in 15 mM Tris-Cl, 150 mM NaCl, pH 7.5, at 4°C.

Fluorescence Measurements

Fluorescence emission spectra were performed on a Spex 212 fluorimeter in the ratio mode, using a 10 mm excitation pathlength, 4 mm emission pathlength semi-micro quartz cuvette, unless otherwise noted. Also unless otherwise noted, fluorescence was measured in PBS (10 mM potassium PO_4, 150 mM NaCl, pH 7.2) or in Na acetate buffer (0.1 M acetate, 0.15 M NaCl, pH 4.5). All experiments were performed at room temperature.

Measurement of CB and MPT fluorescence intensity was performed at excitation and emission λ_{max}. These values are 385 nm and 417 nm, respectively, for the CB-dextrans and 405 nm and 433 nm, respectively, for MPT (emission λ_{max} for these compounds was the same at both pH 4.5 and pH 7.0). CB emission spectra were measured using an excitation wavelength of 370 nm. For both spectra and intensity measurements 2.5 mm slits were generally used. For LRB-SO_2Cl, rhodamine-PE and rhodamine-labeled toxin the excitation and emission wavelengths were 565 nm and 585 nm, respectively. Slits of 5 mm were used. Fluorescence emission spectra of LRB-SO_2Cl and LRB-labeled toxin were measured using an excitation wavelength of 550 nm. Protein fluorescence was monitored with excitation at 280 nm and emission wavelength at 335 nm using 2.5 mm slits.

For all fluorescence experiments (except gel filtration chromatography) background samples were prepared without fluorophore, and where the background fluorescence was significant, it was subtracted to yield the final value.

Purification of CB-Labeled Dextrans

To obtain dextrans of relatively homogeneous size the commercial 3 kD, 10 kD and 70 kD dextrans were fractionated using gel filtration chromatography. Stock solutions of 3 kD, 10 kD and 70 kD CB-labeled dextrans were prepared at 5.0 mg/ml. Then 1 ml of each dextran was loaded on a Sephacryl S-200 column (0.5 cm × 40 cm) and eluted with PBS pH 7 at room temperature. Fractions of 1 ml were collected. Dextran elution was monitored by CB fluorescence using 1.0 mm slits. The four peak fractions were pooled and 1 ml of each pool was rechromatographed on the same column after prewashing with several column volumes of PBS pH 7. The three peak fractions from the rechromatography step were pooled (3 ml total) and used in subsequent experiments. Dextrans were stored at room temperature in the PBS pH 7. The 70 kD dextran exhibited some degradation to lower molecular weight species upon long (over 2 weeks) storage. Therefore, it was used within 2 weeks of purification. The other dextrans did not exhibit this behavior.

Purified CB-Dextrans Have Hydrodynamic Radii Comparable to Proteins of Similar Molecular Weight

To compare the hydrodynamic radii of dextrans to proteins, cytochrome C (M_r 12,348), and BSA (M_r 60,000) dissolved in PBS pH 7

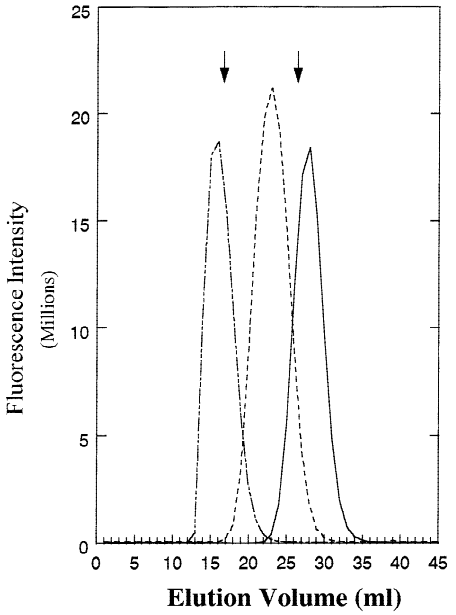

Fig. 1. Elution profile for chromatography of purified CB-labeled dextrans on Sephacryl S-200. Elution of 3 kD (solid lines), 10 kD (dashed lines), and 70 kD CB-dextran (dotted lines) is shown. Arrows indicate the position of elution peaks for BSA (at 18 ml) and cytochrome C (at 26 ml).

were chromatographed using the Sephacryl S-200 column (0.5 cm × 40 cm) and eluted with PBS at room temperature. Fractions of 1 ml were collected. The elution profile of the cytochrome C was followed by measuring absorbance at 409 nm on a Beckman 650 spectrophotometer, and that of BSA by Trp fluorescence. Figure 1 shows cytochrome C gave maximum elution at 26 ml which was comparable to elution at 24 ml for the purified 10 kD dextran, and BSA eluted at 18 ml, which was comparable to 16 ml for the purified 70 kD dextran. This demonstrated that the CB-dextrans have hydrodynamic radii similar to those of proteins with equivalent molecular weights.

Dextran Quenching by Antibodies

To measure binding of CB-labeled dextrans by anti-CB antibodies a 5 μl aliquot of the concentrated anti-CB stock solution (2.5 mg/ml in PBS pH 7.2 with 0.02% NaN_3) was diluted with 500 μl of either PBS pH 7.2 or acetate buffer pH 4.5 at room temperature. Aliquots of 5 μl from a 5 μg/ml stock solution of the crude 3 kD dextran were titrated into the antibody-containing solution at room temperature. Approximately 1 min after each addition fluorescence was measured. These experiments were performed at numerous pHs between pH 3.0 and 7.2, and for each of the dextrans and MPT.

The kinetics of anti-CB binding to CB-labeled dextrans in solution were studied by preparing a solution of 0.03 μM of the crude 3 kD CB-dextran in 1 ml of either PBS pH 7.2 or acetate buffer pH 4.5. The sample was placed in a cuvette and fluorescence was measured before and various times after addition of 5 μl from the anti-CB stock solution.

Calculation of Association Constant for Cascade Blue Binding to Antibody

The apparent dissociation constant for Cascade Blue interaction with antibody was calculated from the formula $K_d = (CB)(Ab)/(CBAb)$. Where (CB) is the concentration of free Cascade Blue, (Ab) is the concentration of free CB binding sites on anti-CB antibodies, and (CBAb) is the concentration of CB bound to Ab. Where quenching is half maximal, the concentration of bound CB-dextran (CBAb) and free CB-dextran (CB) is equal and $K_d = (Ab)$. Since the amount of (Ab_{total}) is known, and $(Ab) = (Ab_{total}) - (CBAb)$, an upper limit to K_d can be estimated, using the total antibody concentration as an upper limit to the concentration of CB-binding antibodies, and taking the number of CB groups per dextran reported by the manufacturer into account.

Entrapping Dextrans Within Model Membrane Vesicles

CB-labeled dextrans (3 kD, 10 kD, or 70 kD) were trapped inside large unilamellar vesicles (LUVs) formed by octyl glucoside dialysis [21] at room temperature. The LUVs were composed of either 20% DOPG/80% DOPC (PG/PC), DOPC (100% PC), or 20% DOPG/30% cholesterol/50% DOPC (PG/cholesterol/PC) (mol/mol). In addition, the samples contained 0.02 mol% rhodamine-PE as a fluorescent marker used to assay lipid concentration. Prior to dialysis total concentration was 10 mM. Initial dextran concentrations of up to 0.03 mM were used. (Dextran concentrations were determined using a CB fluorescence *vs.* concentration curve.) Dialysis tubing (Spectra/Por) with a molecular weight 1,000 cutoff was used. Free dextran was separated from vesicle trapped dextran by filtration on a Sepharose 4B-CL gel filtration column (0.5 cm × 40 cm) at room temperature. Samples were eluted from the column with PBS pH 7.2, and the fractions containing lipid were pooled. CB-dextran concentration was monitored to determine trapping efficiency. From CB fluorescence measurements trapping efficiencies were found to be between 5–7%. This corresponds to vesicles with an average diamter of approximately 1,400 Å. The final concentration of lipid was 2–4 mM. Dextran-containing vesicles (DCV) were stored in the PBS 7.2 buffer at room temperature. The CB-dextrans remained entrapped inside the LUVs for a period of 2 weeks as determined by the lack of CB quenching (<5%) upon antibody addition in the absence of toxin.

MPT-containing vesicles were made with the same innitial trapping protocol, but in the dialysis step a concentration of MPT equal to that in the sample was included in the external dialysis buffer in order to maximize MPT trapping. Passive leakage of MPT was also slow, but significant with leakage of about 50% of the MPT within a period of 1 week. Once vesicles were formed and the free MPT was separated from trapped MPT using the Sepharose 4B-CL column, the vesicles were used within 24–48 hr. As a further control, baseline MPT leakage was measured from the amount of quenching observed in trapped MPT samples in the absence of toxin.

Dextran Leakage Assay

The kinetics of dextran leakage were measured by diluting an aliquot (25–45 μl) of vesicles containing entrapped CB-labeled dextran to 550 μl with pH 4.5 acetate buffer at room temperature. Fluorescence was measured, the sample transferred to a test tube, and either 1, 5 or 10 μg of toxin was then added. After the samples were vortexed vigorously for 20 sec[1] they were then transferred back to the semi-micro cuvette and the fluorescence measured at various time intervals. Control experiments showed that the PBS did not significantly affect final pH

[1] Vigorous mixing during the incubation was necessary to achieve rapid quenching. Otherwise, artificially long incubation times (up to 30 min) were needed to obtain maximal quenching.

(which was close to 4.5), even when equal volumes of PBS and the acetate buffer were mixed.

Measurement of the effect of pH or toxin concentration on the amount of CB efflux were performed as follows: an aliquot (25–45 μl) of vesicles with entrapped CB-labeled dextran or MPT was added to 150 μl of pH 4.5 acetate buffer at room temperature. Then a small aliquot (2.5–10 μl) was added from one of various PBS diluted stock solutions of toxin with different concentrations. Samples were incubated for 30 min and then the volume was increased to 500 μl with pH 4.5 acetate buffer. The final lipid concentration was 200 μM and the final pH 4.5. Next, CB fluorescence was measured followed by addition of excess anti-CB antibody, i.e., sufficient to obtain maximal quenching (2–5 μl of a 2.5–2.8 mg/ml stock solution). The fluorescence was remeasured after 5 min. The percent quenching was calculated as follows: [1 − {(fluorescence + Ab)/(fluorescence − Ab)}] × 100% in a sample containing toxin − [1 − {(fluorescence + Ab)/(fluorescence − Ab)}] × 100% in a sample lacking toxin, and then percent of maximum quenching was calculated by dividing the percent quenching by the amount of quenching obtained in the presence of enough octyl glucoside (10 μl of a 200 mg/ml stock solution in PBS) to disrupt the vesicles and thereby release all entrapped molecules. Control experiments showed octyl glucoside did not interfere with quenching of CB-dextrans in solution. It should be noted that the subtraction of quenching in the absence of toxin results in an underestimate of % release. This was significant only in the case of MPT.

Experiments at constant toxin concentration were performed by diluting various aliquots of a vesicle preparation containing 2.9 mM lipid and entrapped 10 kD dextran to 500 μl with pH 4.5 acetate buffer. A 2 μl aliquot of toxin (0.1 mg/ml) was added to each sample. Samples were incubated for 30 min and then fluorescence was measured before and after addition of an aliquot of anti-CB from the stock solution sufficient for maximal quenching (1–10 μl). The final lipid concentrations in the samples were 0, 4, 5.3, 8, 40, 53, 80, 400, 533 and 800 μM.

Toxin titration experiments were performed by diluting an aliquot from a 2.8 mM lipid vesicle sample containing entrapped 10 kD dextran to 500 μl with pH 4.5 acetate buffer (giving a lipid concentration 200 μM), and then adding 5 μl (12.5 μg) of anti-CB antibody. Fluorescence was measured, and then toxin was added to the sample in 1 μl aliquots (from a 0.5 mg/ml stock). After each addition of toxin the samples were vigorously vortexed and after a 2 min incubation the fluorescence was remeasured.

Assay of Vesicle Fusion by Diphtheria Toxin

Vesicle fusion was assayed by measurement of lipid mixing. A 10 mM stock concentration of LUVs composed of 18% DOPG/78% DOPC and containing 2% rhodamine-PE and 2% NBD-PE or composed of 19.8% DOPG/79.8% DOPC and containing 0.2% rhodamine-PE and 0.2% NBD-PE (mol/mol) were prepared by mixing the appropriate amounts of the lipids, drying for 1 hr at high vacuum, suspending in PBS, and after a freeze thaw cycle, 21 extrusions through 10 nm filters using a LipsoFast extruder (Avestin, Ottawa, Canada).

For fusion assays 1.1 μl of the LUVs containing 2% rhodamine-PE and 2% NBD-PE were diluted to 550 μl with pH 4.5 buffer. This yields a concentration of 20 μM lipid. An aliquot (4.12 μl) of PG/PC LUVs containing only labeled lipid was added to the sample so as increase lipid concentration to 200 μM (i.e., there was a 1:10 ratio of labeled vesicles to total vesicles). The kinetics of fusion were assayed after adding 10 μg toxin to the samples, and vortexing for 10 sec, by measuring the NBD fluorescence at various time points. NBD fluorescence was mesured using an excitation wavelength of 470 nm and an emission wavelength of 530 nm using 1.0 mm slits in the direction of excitation and 3.0 mm slits in the direction of emission.

Upon fusion of labeled and unlabeled vesicles, the NBD and rhodamine concentrations within the bilayer are reduced, which decreases NBD to rhodamine energy transfer. As a result, NBD fluorescence increases. The fluorescence increase upon total mixing of the lipids in the labeled and unlabeled vesicles was estimated to be 10-fold, as determined by comparing the fluorescence of a sample containing 200 μM lipid with 0.2% NBD-PE and 0.2% rhodamine-PE to that in a sample with 2% of the labeled lipids. Under the assay conditions used 90% of the first fusion events with a labeled vesicle involve fusion with an unlabeled vesicle. Thus the first round of fusion dilutes NBD and rhodamine by a factor of about two. Because energy transfer resulting from acceptor molecules randomly distributed in membrane is roughly exponential in acceptor (rhodamine) concentration [6], this yields a rough estimate of a threefold increase in NBD fluorescence after the first round of fusion.

Crosslinking Experiments

A fresh 25 mM stock solution of DSP or DST in dimethylformamide (DMF) was prepared. Crosslinking of monomer toxin was performed by adding 10 μl of the DSP or DST stock solution to samples containing 10 μg toxin in 200 μl buffer solution pH 7 in the presence of LUVs containing 200 μM lipid composed of either 20% DOPG/80% DOPC or 20% DOPG/30% cholesterol/50% DOPC. Samples were incubated for 2 hr at room temperature, and then an aliquot subjected to SDS-PAGE using Pharmacia precast 4–15% gradient gels. Electrophoresis was carried out on the Pharmacia Phastsystem (Pharmacia Biotech, Piscataway, NJ) [21], and the gels visualized by silver staining. To demonstrate that the reaction with the crosslinker took place during the 2 hr incubation period, a sample of crosslinker was incubated for 2 hr in the presence of pH 4.5 buffer before toxin was added. Immediately after toxin addition an aliquot of the sample was removed and subjected to electorphoresis. Under these conditions no crosslinking was observed.

Rhodamine Labeling of Toxin

Monomer diphtheria toxin was labeled by mixing 3 mg diphtheria toxin (from a stock solution of about 12 mg/ml) with 3 mg LRB-SO_2Cl/celite and enough 50 μM sodium carbonate buffer pH 9.2 to bring final volume to 1 ml. The sample was incubated with shaking for 45 min at room temperature and then centrifuged in a microcentrifuge for 15 min to pellet the celite suspension. The free rhodamine remaining in the supernatant was removed from the rhodamine-labeled toxin by chromatography of the supernatant on a Sephadex G-50 gel filtration column (0.5 cm × 15 cm) at room temperature. The labeled toxin was eluted from the column with PBS pH 7.0. The amount of labeling was estimated (assuming ϵ was not affected by labeling) by measuring the amount of rhodamine absorbance (using $\epsilon_{565nm} = 85{,}000\ cm^{-1}\ M^{-1}$) in the fractions containing the labeled protein. Toxin concentration was calculated both from absorbance at 280 nm ($A_{(1cm)} = 1.06$ for 1 mg/ml) [3] and from Coomassie plus assay (Pierce Chemical). The estimated final ratio of rhodamine label to toxin was generally close to 1:1 (mole/mole).

Measurement of Toxin Oligomerization by Rhodamine Self-Quenching

LUVs (PG/PC or PG/cholesterol/PC) without trapped dextran were prepared by octyl glucoside dialysis (without the final chromatography step, and using trace pyrene-PE to follow lipid concentration). Assuming no loss during dialysis 10 mM lipid LUVs were prepared in 1 ml PBS.

An aliquot of unlabeled toxin (0–45 μl) was added to samples containing a 11 μl aliquot of the LUVs, and then an aliquot of labeled toxin (10–50 μl) was added such that the desired ratio of labeled to unlabeled toxin was obtained while fixing total toxin in each sample at 5 μg. Acetate buffer pH 4.5 or PBS 7.2 was added to each sample for a final volume of 550 μl. This gave a final lipid concentration of 200 μM. Relative rhodamine self-quenching in a sample with x% of the protein from the rhodamine labeled population was calculated after normalizing fluorescence to that for an equal number of labeled toxin molecules as follows: ([Fluorescence in the sample with x% toxin from the labeled population/Fluorescence in a sample with 10% toxin from the labeled population].

Similar rhodamine self-quenching experiments were performed using a fixed amount of labeled toxin. In these experiments each sample contained 5 μg of rhodamine-labeled toxin and various amounts of unlabeled toxin such that the labeled toxin varied between 10% and 100% of total toxin concentration. Rhodamine self-quenching was measured both in pH 4.5 acetate buffer and PBS pH 7.2 in the presence of PG/PC LUVs (with 200 μM lipid). The percent of relative rhodamine self-quenching was calculated by dividing the fluorescence in a sample with x% toxin from the labeled population by the fluorescence measured in the sample with 10% toxin from the labeled population and multiplying this ratio by 100%.

Results

Fluorescence Quenching Assay For Pore Formation: The Binding of Anti-Cascade Blue Antibodies to Labeled Dextrans is Rapid, Tight and Independent of pH

Toxin-mediated pore formation was characterized using a novel fluorescence quenching assay. This assay measures the leakage of Cascade Blue (CB) labeled dextrans or the free Cascade Blue dye, MPT, out of the lumen of large unilamellar vesicles (LUVs) through the quenching of CB fluorescence by ant-CB antibodies added to the external solution. Anti-CB blue antibodies efficiently (up to 80–90%) and rapidly ($t_{1/2}$ < 5 sec) quenched 3 kD CB-dextran fluorescence both at pH 7 and 4.5 (Fig. 2).[2] Similar results were obtained for the 10 kD and 70 kD dextrans.

CB-labeled dextran was titrated into solutions containing anti-CB antibody to determine the conditions (excess antibody) under which quenching can be used to measure the release of CB-dextran from vesicles (Fig. 3). For the 3 kD dextran, 25 μg/ml of anti-CB is sufficient to assay release of up to 0.06 μM CB-dextran. Similar values were obtained for the other CB-dextrans and MPT (*not shown*). From this experiment, K_d for 3 kD CB-dextran binding to anti-CB antibody was estimated to have an upper limit of <0.3 μM at pH 4.5 and 7 (*see* Materials and Methods). Similar limits for K_d were found for the other CB-dextrans and MPT at various pH values between 3.5 and 7 (*data not shown*).

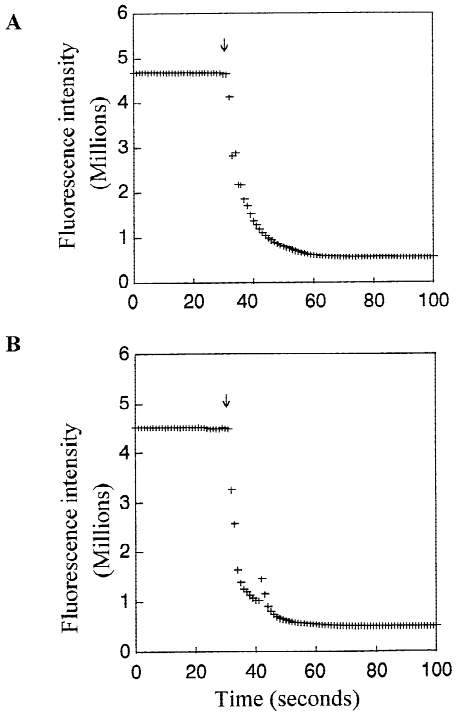

Fig. 2. Kinetics of 12.5 μg/ml α-CB binding to 0.03 μM 3 kD CB-dextran. CB-dextran fluorescence at (*A*) pH 7.0 or (*B*) pH 4.5 is shown. The arrow designates the time at which antibody was added to the sample. Readings were taken at 1 sec intervals.

Diphtheria Toxin-Mediated CB-Dextran Release Occurs at Low pH

Based on the information above, the quenching assay was applied to the study of pore formation by diphtheria toxin. Figure 4 shows the effect of pH on the ability of toxin to release LUV-entrapped 3 kD CB-dextran. Using individual samples, the pH at which toxin was added to the dextran-containing vesicles (DCVs) was varied. Release from vesicles with three different lipid compositions, 20% PG/80% PC, 20% PG/30% cholesterol/50% PC, and 100% PC, was compared. The effect of toxin was similar for all three lipid compositions. When toxin was added to DCVs above pH 5.5 the dextran fluorescence was not quenched, i.e., there was no release of CB-dextran. Below pH 5.5 incubation of the toxin with DCVs caused the dextrans to be quenched maximally, i.e., the CB-dextran was fully released. The transition pH for release was close to 5.2. This pH is in agreement with previous studies showing that the toxin undergoes partial unfolding [3], and inserts into lipid vesicles, in the range pH 5–5.5 [10]. These data also agree with studies

[2] In addition, the fluorescence emission λ_{max} shifted 7 nm towards the blue end of the spectrum (*data not shown*).

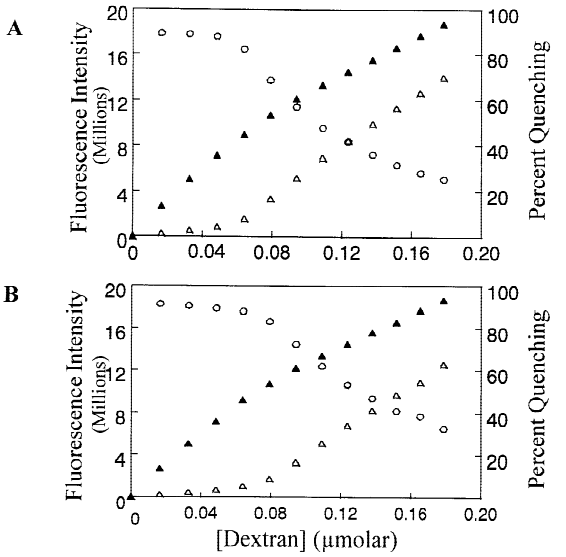

Fig. 3. Fluorescence quenching assay of binding of α-CB antibodies to 3 kD CB-dextran in solution. Fluorescence of various concentrations of CB-dextran at (*A*) pH 7.0 or (*B*) pH 4.5 is shown: (▲) in the absence of antibody; or (△) in the presence of 25 μg/ml antibody. (○) % fluorescence quenching by antibody.

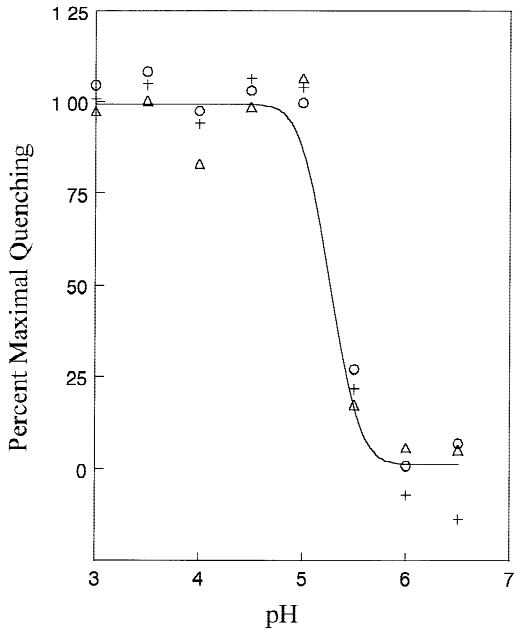

Fig. 4. The dependence of release of 3 kD CB-dextran from DCV on pH. Quenching of 3 kd CB-dextran entrapped in LUVs composed of (+) 20% PG/80% PC (mol/mol), (△) 20% PG/30% cholesterol/50% PC, or (○) 100% PC by 10 μg toxin is shown. Samples contained a final concentration of 200 μM lipid in a total volume of 500 μl. Buffers at pH 6.0 and above were 100 mM potassium phosphate, 150 mM NaCl. Buffers below pH 6.0 consisted of 100 mM sodium acetate, 150 mM NaCl.

showing that pore formation occurs when toxin inserts at low pH [20], and thus confirms that CB-dextran release assayed by antibody binding is able to detect toxin-mediated pore formation.

Toxin-Mediated CB-Dextran Release is Rapid at Low pH, and Involves Pore Formation

The rate of toxin-mediated release of the CB-dextrans at low pH was also examined (Fig. 5). Release of MPT by 10 μg toxin was rapid, and complete within 30 sec. Release was slightly less rapid for the 3 kD dextran, with $t_{1/2}$ = 2 min and complete release within 10 min, and even less rapid for the 10 kD dextran with $t_{1/2}$ = 5 min and complete release within 20 min. At lower toxin levels (1.0 μg and 5.0 μg), the rate of release was slightly slower, but nearly leveled off within 30 min (*not shown*).

Since diphtheria toxin can cause membrane aggregation and fusion, the possibility that the leakage of entrapped molecules involves some sort of transient event rather than a toxin-induced pore had to be considered. The difference in the kinetics of release as a function of the size of entrapped molecules (Fig. 5*A*), and the limited size of entrapped molecules that can be released (*see below*), rule out toxin-induced vesicle lysis as the mode of dextran release.

In addition, the kinetics of the release of entrapped materials was much more rapid than the rate of fusion, which only resulted in less than one fusion event per vesicle even after 30 min (Fig. 5*B*). This rules out leakiness directly associated with fusion events. Finally, experiments using entrapped antibody were performed to examine transient leakiness. In this protocol CB-dextrans are added externally and their movement into vesicles is measured. (The antibodies are too large to leak from the vesicles, as shown by experiments described below, and centrifugation studies (*not shown*).) Using this system the entry of the 10 kD CB-dextran into the vesicles was as rapid, or even more rapid, when CB-dextran was added about 1 hr after addition of the toxin than when it was added before the toxin (*data not shown*). If the toxin induced only transient leakiness, then there should have been no entry of CB-dextran into the vesicles when it was added 1 hr after toxin. We conclude that the movement of CB-dextrans across membranes induced by toxin addition involves pores formed by the toxin molecules.

Dextran Leakage by Diphtheria Toxin at Low pH Depends on Toxin Concentration

The extent of dextran release as a function of toxin concentration was examined in order to determine whether pore size was affected by toxin concentration. Toxin amounts were varied over a wide range, 0.025 to 10 μg

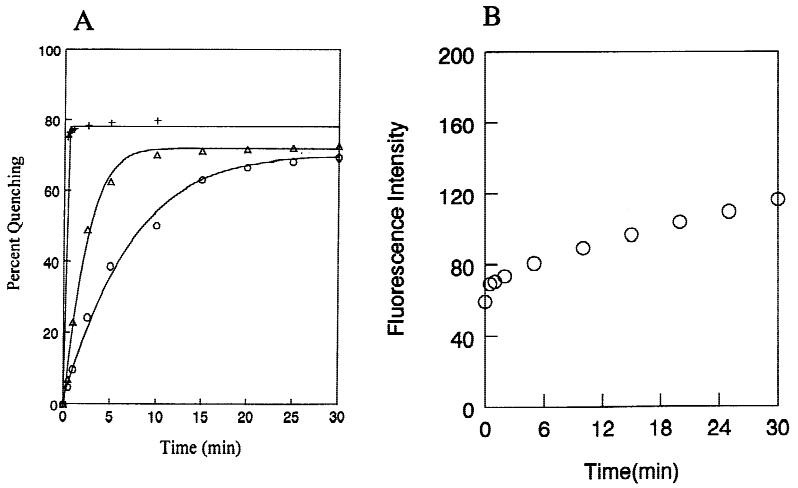

Fig. 5. (*A*) Kinetics of toxin-induced efflux of CB-dextran entrapped in 200 μM PG/PC LUVs at pH 4.5. The rate of release by 10 μg toxin is shown for: (+) MPT, (△) 3 kD CB-dextran, and (○) 10 kD CB-dextran. Sample volume was about 550 μl (see Materials and Methods for details.). (*B*) Kinetics of toxin-induced fusion of 200 μM PG/PC LUVs at pH 4.5, as assayed by the increase of NBD fluorescence upon the fusion of vesicles induced by the addition of 10 μg toxin. Sample volume was about 550 μl. The twofold increase in NBD fluorescence after 30 min of incubation with toxin corresponds to less than one fusion event per vesicle (*see* Materials and Methods for details).

(i.e., an initial ratio of about 0.65 to over 250 toxin molecules/vesicle[3]). Figure 6*A* illustrates toxin-mediated dextran release from PG/PC vesicles as a function of the amount of toxin present. The small molecule MPT was already partly released at the lowest toxin concentrations and its release plateaued at 0.25 μg. In contrast, significant release of the larger CB-dextrans was not observed at 0.25 μg. Half maximal release (R_{50}) of the 3 kD CB-dextran occurred at about 0.5 μg toxin. Higher toxin levels were needed to release the 10 kD CB-dextran (R_{50} = 2.5 μg). The 70 kD was not significantly released even at the highest toxin concentrations. (The lack of 70 kD dextran release demonstrates that the pore size is limited, in agreement with previous studies [20, 21].) Thus, the larger the trapped molecule, the higher the toxin concentration needed for release. This suggests that the pore size is increasing as toxin concentration increases. An alternate possibility is that the differences in the concentration dependence of release for the different CB-dextrans and MPT reflect a differing concentration dependence of the kinetics of release, due to increasing numbers of pores as toxin concentration is increased, rather than differing pore size. This possibility was ruled out by experiments in which the toxin concentration dependence of 3 kD and 10 kD dextran release after 30 min was compared to that at 24 hr. These experiments showed a 2–4 fold decrease in the concentration of toxin allowing half maximal release, but a significant difference was still observed between R_{50} values for the dextrans (*not shown*). Furthermore, even after overnight incubation, release of 3 kD and 10 kD CB-dextrans required severalfold higher toxin levels than the release of MPT in 30 min. If an increase in toxin concentration increased pore number rather than pore size, then the different size dextrans and MPT should have exhibited equal R_{50} values after the overnight incubation. We conclude the size of the pore formed by the toxin must increase as toxin concentration is increased.

[3] This is the initial ratio. Since the toxin has fusogenic activity, the number of vesicles decreases after toxin addition [4, 12].

Lipid Composition Effects

The effect of lipid composition on toxin-mediated pore formation was also examined (Fig. 6*B* and *C*). As in the PG/PC vesicles, the larger the trapped molecule, the greater the toxin concentration required for release. The amount of toxin required to release CB-dextrans was similar in PG/PC and PC DCVs, although more toxin was needed to release MPT in the latter case. However, in PG/cholesterol/PC vesicles, significantly less toxin was needed to achieve release, with about 5-fold less toxin needed for half maximal release for the 3 kD and 10 kD CB-dextran. These differences could be due to several factors, but in any case show that the basic behavior of the toxin is similar in all three lipid compositions.

Pore Size Reflects the Concentration of Toxin Within the Membrane

The observation that pore size gradually increases as toxin concentration increases implies toxin oligomerization is involved, and that the larger the oligomer the larger the pore size. Two possible mechanisms for oligomerization are (i) oligomers pre-form in aqueous solution so that oligomer size is fixed by the concentration of toxin in solution, or (ii) oligomer size is determined by the concentration of toxin within the bilayer (i.e., toxin: lipid ratio). To distinguish between these possibilities

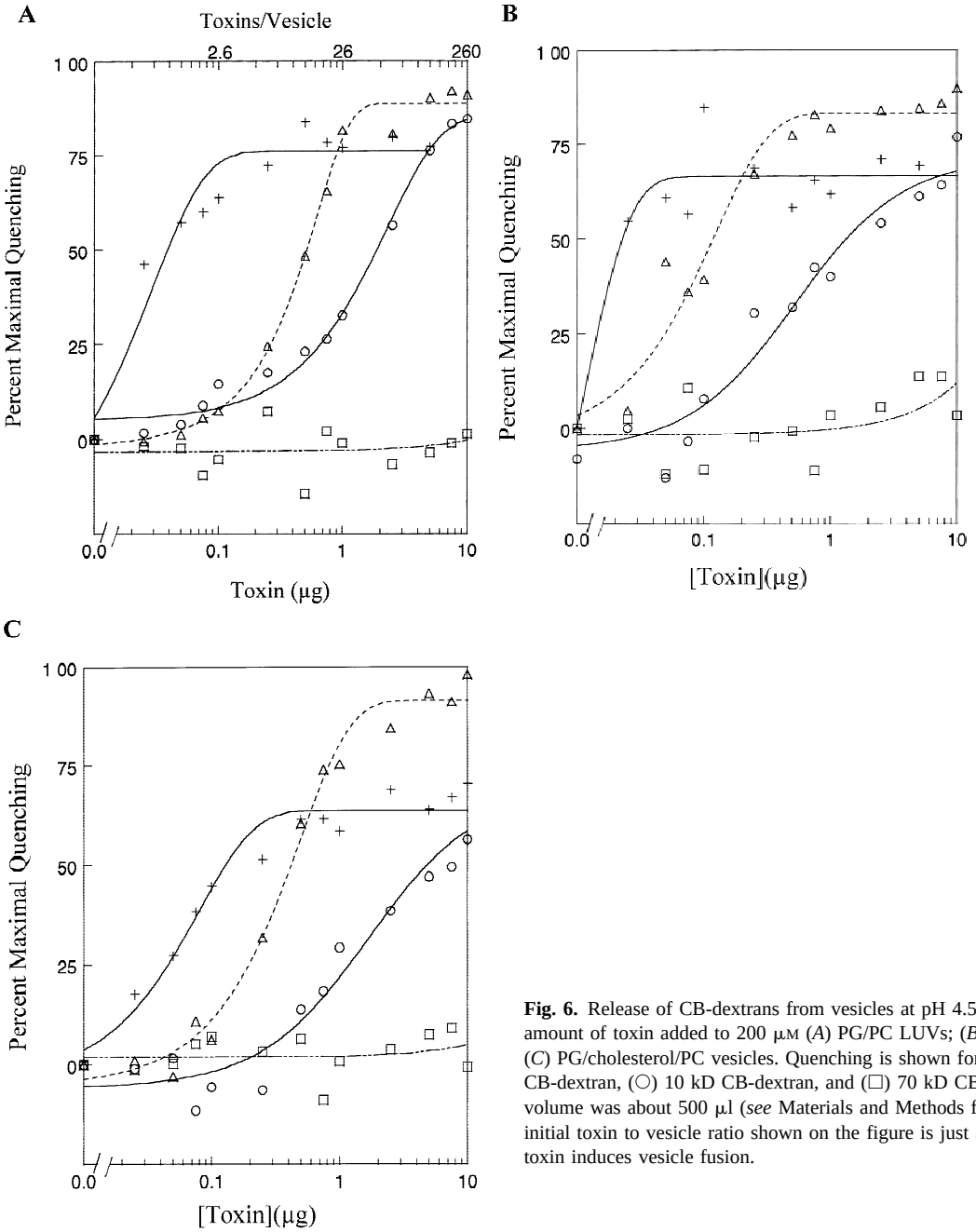

Fig. 6. Release of CB-dextrans from vesicles at pH 4.5 as a function of the amount of toxin added to 200 μM (*A*) PG/PC LUVs; (*B*) 100% PC vesicles; or (*C*) PG/cholesterol/PC vesicles. Quenching is shown for (+) MPT, (△) 3 kD CB-dextran, (○) 10 kD CB-dextran, and (□) 70 kD CB-dextran. Sample volume was about 500 μl (*see* Materials and Methods for details). Note that the initial toxin to vesicle ratio shown on the figure is just a rough guide, as the toxin induces vesicle fusion.

dextran leakage was measured under different conditions.

In one experiment the lipid concentration was varied instead of toxin concentration. The absolute toxin concentration used was insufficient to allow release of the 10 kD dextran from 200 μM lipid DCV (Fig. 6). If the concentration of toxin in solution determines oligomer size, then this experiment should have resulted in oligomers (and pores) of a constant size too small to allow release of the 10 kD dextran. Instead, 10 kD dextran release was observed with the same dependence on toxin:lipid ratio as in samples in which toxin concentration was varied (Fig. 7). This behavior is what would be expected if the concentration of toxin in the membrane determines oligomer (and pore) size.

In the second experiment, toxin concentration was increased by adding a series of aliquots to a single sample of vesicles, with sufficient time between additions to allow membrane insertion by the toxin (which is a rapid process [10, 17]). This protocol used the same amount of toxin (0.5 μg) in each aliquot. This amount of toxin was chosen because because a single 0.5 μg aliquot

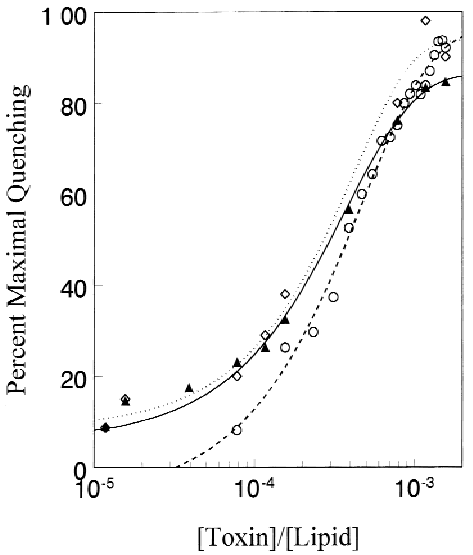

Fig. 7. Release of 10 kD CB-dextran as a function of toxin/lipid molar ratio for samples prepared by different methods. (◇) Various concentrations of PG/PC LUVs containing entrapped 10 kD-dextran incubated with 0.2 μg toxin. (▲) Various concentrations of toxin incubated with 200 μM PG/PC LUVs containing entrapped 10 kD-dextrans. (○ Titration of 200 μM PG/PC LUVs containing entrapped 10 kD-dextran with 0.5 μg aliquots of toxin. See Materials and Methods for details.

is insufficient to form pores large enough to release a 10 kD dextran (Fig. 6). If the toxin oligomerizes only in solution then successive additions should not have increased pore size, and pores should have remained too small to allow 10 kD dextran leakage. Instead, as the total amount of toxin increased, increasing leakage of the 10 kD dextran was observed, with a dependence on toxin concentration similar to that in the other protocols[4] (Fig. 7). This result not only confirms that the concentration of toxin in the membrane regulates pore size, it also suggests that the toxin added in later aliquots could interact with the previously inserted toxin molecules to form a larger pore. The ability of toxin molecules added to solution to interact with toxin molecules that have previously been membrane inserted has also been observed with the isolated T domain [42].

Potential Diphtheria toxin Oligomerization Can Be Detected by Chemical Crosslinking

The dependence of pore size on toxin concentration suggests a dependence on toxin oligomerization. To examine whether oligomers could be observed directly,

[4] The slight difference seen probably arises from the fact that the time between readings in the titration experiment was too short to allow maximal release of 10 kD dextran.

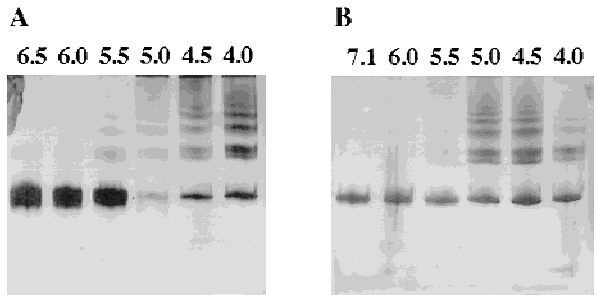

Fig. 8. Crosslinking of diphtheria toxin at various pH in the presence of PG/PC vesicles. Gels are shown for: (*A*) crosslinking with DSP; and (*B*) crosslinking with DST. pH values are shown on gels.

chemical crosslinking by the homobifunctional amine reactive crosslinker DSP was measured as a function of pH. Diphtheria toxin in PG/PC vesicles was incubated in the presence of DSP and then subjected to SDS-PAGE. Figure 8*A* shows that crosslinking occurred only at low pH, where the toxin becomes hydrophobic and inserts into the membrane bilayer [10, 17, 31, 33, 44, 45][5]. At low pH a ladder of bands was observed. This could suggest that toxin oligomerization may not be restricted to a single stoichiometry, consistent with the pore size results, but also could be due to the inefficiency of the crosslinking process. There was no observable difference between the crosslinking pattern in PG/cholesterol/PC vesicles and that in PG/PC vesicles (*data not shown*).

A second amine-reactive homobifunctional crosslinker, DST, was used to confirm that crosslinking was not an artifact of the crosslinker used. DST has a shorter spacer arm (6.4 Å) than DSP (12 Å). A similar pattern of crosslinking was seen although the efficiency of crosslinking was less (Fig. 8*B*).

Detection of Toxin Oligomers Using Fluorescence Self-Quenching

Although crosslinking is useful for detecting protein–protein interactions, artifacts may arise due to crosslinking during collisions between protein molecules in the membrane. This could significantly exaggerate the apparent degree of oligomerization, and thus crosslinking experients of this type cannot be definitive. Therefore, we also used a fluorescence quenching assay which is not affected by such transient contacts. In this method, oligomerization was detected by the self-quenching of

[5] Control experiments showed that the reason the conformational transition pH was slightly elevated (to pH 5.5) in the crosslinking samples relative to that previously determined by fluorescence (about pH 5) [3] was due to the presence of the 5% (v/v) dimethylformamide used to dissolve the crosslinker.

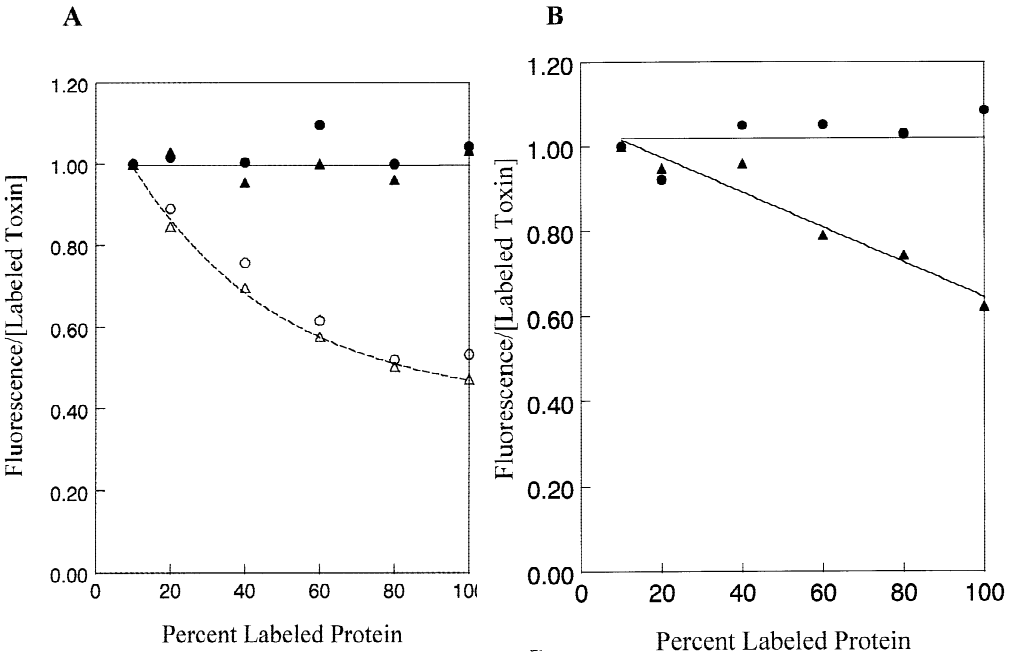

Fig. 9. Detection of diphtheria toxin oligomerization by self-quenching using rhodamine-labeled toxin. (*A*) The amount of rhodamine quenching is shown for samples containing a 9 μg/ml total diphtheria toxin in the presence of 200 μM lipid (circles) PG/PC LUVs, or (triangles) PG/cholesterol/PC LUVs, at neutral pH (filled symbols) or at low pH (open symbols). (*B*). As in (*A*) for PG/PC LUV except total toxin was varied with the amount of labeled toxin fixed at 9 μg/ml. Circles, pH 7. Triangles, pH 4.5.

fluorescent groups attached to protein. This quenching occurs when fluorescently labeled molecules are in close proximity [7, 26, 38]. If a protein forms oligomers, then there will be self-quenching in those oligomers containing more than one fluorescently labeled protein molecule. The amount of self-quenching can be determined by comparison to the fluorescence in a reference sample in which there is excess unlabeled protein. Inclusion of excess unlabeled molecules abolishes self-quenching by diluting the labeled molecules such that few oligomers have more than one labeled protein molecule.

Self-quenching of fluorescein was previously used to study the oligomerization of the cytolytic protein complement C9 [38, 39]. In this report lissamine rhodamine was used in place of fluorescein. This rhodamine does not exhibit pH-dependent fluorescence properties over the range of pH 4–8 (*data not shown*), presumably because it does not contain the ionizable groups (carboxyl and aromatic hydroxyl) found on fluorescein. Previous studies from our lab have shown self-quenching of rhodamine-labeled toxin can be observed at low pH [9].

Figure 9 shows the effect of the ratio of unlabeled to labeled toxin on rhodamine fluorescence for toxin incubated with PG/PC or PG/cholesterol/PC vesicles. As expected, at pH 7, where the toxin is hydrophilic [3], there was no quenching, indicating no oligomerization. In contrast at low pH there was increasing self-quenching as the fraction of labeled toxin was increased. Self-quenching was observed at low pH both when maintaining a constant total toxin concentration (Fig. 9*A*), and when maintaining a constant labeled toxin concentration but adding different amounts of unlabeled toxin (Fig. 9*B*)[6]. This latter experiment rules out the possibility that

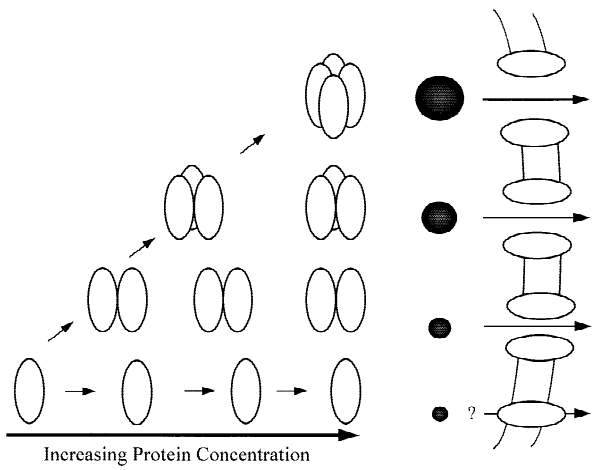

Fig. 10. Model for diphtheria toxin aggregation and pore formation behavior. As toxin concentration increases larger oligomers forming larger pores (shown in schematic cross section) are present.

[6] The apparent difference in fluorescence at 100% rhodamine labeled toxin in Figs. 9*A* and *B* at pH 4.5 is due to the normalization to equivalent values at 10% labeled toxin. The actual absolute fluorescence is the same at 100% labeled toxin.

self-quenching at low pH arises from toxin molecules that are close to one another simply by virtue of their being randomly distributed in the bilayer. If that had been the case, addition of unlabeled protein, which should not significantly dilute the density of labeled toxin in the bilayer, should not have abolished self-quenching. The possibility that a change in light scattering upon addition of unlabeled toxin affects fluorescence was ruled out by the observation that in vesicles in containing rhodamine-labeled PE instead of labeled toxin, rhodamine fluorescence was unaffected by the addition of the amounts of toxin used in the toxin self-quenching experiments (*not shown*).

Discussion

Diphtheria Toxin Pore Properties

Previous studies have provided a complex picture of diphtheria toxin pore formation. Several (but not all [13]) studies have suggested the toxin can form a large-sized pore [22, 23, 44], although only one study directly observed leakage of materials of high molecular weight (>5000) [20]. Both linear and nonlinear dependencies of pore-dependent flux on toxin concentration have been reported [22, 36] leading to confusion about whether the pore formation is dependent on toxin oligomerization (*see below*). Some of the differences between individual studies may have been due to pH, temperature, and the presence or absence of a pH gradient and/or membrane potential. Indeed, in one study a dependence of apparent pore size on pH was noted [20]. Our report now shows that the concentration of toxin in the membrane is a major variable influencing toxin pore properties, and is likely to have been an important factor in some of the unexplained differences between earlier studies.

Diphtheria Toxin Oligomerization

There has also been no clear picture of diphtheria toxin oligomerization. Some studies have hinted that oligomerization can occur, while others have suggested there is no oligomerization, or a single oligomer size [20, 22, 33]. However, in previous studies oligomerization was often indirectly examined via toxicity, or the amount of photochemical labeling, and we have previously noted these methods can respond to variables other than oligomerization [25]. Dimers formed by domain exchange have been observed in the crystal form of the toxin, but the relationship of these native conformation structures to that at low pH is unclear [2]. Large oligomers of the isolated T domain have been reported in solution at low pH [1], and other evidence for T domain oligomerization in membranes has been obtained [42], but whether whole toxin behaves similarly is uncertain.

There is also little information on diphtheria toxin oligomerization *in vivo*. One study indicated that a single catalytic domain introduced into the cytoplasm is, given a long enough incubation time, sufficient to kill a cell [36], but this does not mean that one toxin molecule kills cells *in vivo.* Another group has presented evidence suggesting that a number of toxins must enter an endosome in order for translocation to occur [18, 19]. Most intriguing are studies on other toxins. It has been found that oligomerization at the cell membrane is a key step in the assembly of the membrne penetrating forms of α-hemolysin [40] and anthrax toxin [29]. This suggests oligomerization of diphtheria toxin at a similar stage of entry into cells would be plausible.

Therefore, it is significant that this study indicates oligomerization of the toxin at low pH can occur within the lipid bilayer, as shown by the increase of pore size as toxin concentration increases, and the observation of self-quenching of fluorescently labeled toxin. The observation that the increase in pore size is gradual can be explained most easily with a model in which toxin oligomer size gradually increases at high toxin concentrations (Fig. 9). In this way the toxin behavior differes from the fixed oligomeric stoichiometries seen in other membrane-inserting toxins, such as staphylococcal α-hemolysin and anthrax toxin [29, 34, 40]. Rather, diphtheria toxin oligomerization appears to be more like that of the pore-forming C9 component of complement which can form pores and oligomers of various sizes [27].

Unfortunately, pore size cannot be used to estimate oligomer size. One reason is that a model in which there is a pore is partly bordered by lipids [20, 27] cannot be ruled out. A second reason is that a calculation of oligomer size from pore size would require an estimate of the thickness of the protein wall surrounding the pore, which is also unknown. The crosslinking and fluorescence quenching assays used here also proved too insensitive to obtain unambiguous information about the dependence of oligomer size on toxin concentration. Therefore, additional studies will be necessary to obtain the exact relationship between a given degree of oligomerization with a particular pore size.

Why Oligomerization May Be Critical For Functional Membrane Insertion

Despite the remaining uncertainties, the evidence in this study for diphtheria toxin oligomerization and its concentration dependence may represent an important clue to how toxin pore properties and translocation across membranes is regulated. A close relationship between

pore formation and toxin translocation has previously been established by a number of studies showing that toxin mutants which fail to form pores, fail to properly insert and translocate into the cellular cytoplasm [14, 37]. Furthermore, we have recently shown that oligomeric interactions between toxin T domains can allow their transmembrane insertion [42]. Thus, it appears that oligomerization is a critical step in toxin insertion and translocation.

Combined with the previous studies on other toxins noted above, this study suggests that oligomerization is likely to be a generally important property for the efficient conversion of proteins that convert from a stable water soluble conformation into a transmembrane conformation. For proteins to fold stably in solution, they must have a hydrophobic core of limited size. Therefore, a medium-sized protein would be expected to have a ratio of hydrophobic to hydrophilic regions lower than that of polytopic transmembrane proteins such as those in the seven-helix receptor class [16]. As pointed out by Papini et al. [33] oligomerization should aid in the efficient burial of hydrophilic sequences. In fact, the larger the oligomer, the smaller will be the ratio of hydrophobic surface facing lipid to total volume needed to achieve transmembrane insertion of the hydrophilic segments. In other words, the larger the oligomer, the lower the fractional content of hydrophobic segments needed in a water soluble monomer to allow transmembrane insertion of the entire protein.

The relationship between oligomerization and transmembrane insertion may be somewhat different for inserting proteins which form transmembrane β sheets, such as the α-hemolysin. Transmembrane β sheets can be composed of relatively short (10–14 residue) strands that only require hydrophobic residues at every other position. Thus, a protein would not have to be especially hydrophobic to have the capacity to form such strands.

The Possible Relationship of Oligomerization and Pore Formation to the Translocation of the A Chain

As noted above, there is strong evidence that pore formation is closely related to the proper transmembrane insertion of the toxin. Therefore, the characterization of the pore-forming properties of the toxin are a critical step in understanding its action. However, it is not yet possible to specify the relationship of pore formation to A chain translocation. At very high concentrations the toxin allows a 10 kD dextran to escape from vesicles, and previous studies demonstrated a 17 kD dextran can also be released [21]. It is not clear whether this means the pore is large enough to allow translocation of the 21 kD A chain. To answer this question directly, it will be necessary to examine the ability of whole toxin molecules to induce the release of vesicle-entrapped isolated A chains. Another way to define the relationship of pore size to translocation will be to compare the concentration dependence of A chain translocation to that of pore size. In any case, the relationship of pore size to toxin oligomerization revealed in this study should be an important clue to our understanding of the translocation mechanism.

The authors would like to thank Dr. Laura Ann Chung who developed the rhodamine self-quenching assay used in these experiments, and Kelli Kachel for performing the experiments measuring dextran release after long incubation times. This work was supported by National Institutes of Health grant GM31986.

References

1. Bell, C.E., Poon, P.K., Schumaker, V.N., Eisenberg, D. 1997. Oligomerization of a 45 Kilodalton Fragment of Diphtheria Toxin at pH 5.0 to a Molecule of 20–24 Subunits *Biochemistry* **36:** 15201–15207
2. Bennett, M.J., Choe, S., Eisenberg, D. 1994. Refined structure of dimeric diphtheria toxin at 2.0 Å resolution. *Protein Sci.* **3:**1444–1463
3. Blewitt, M.G., Chung, L.A., London, E. 1985. Effect of pH on the conformation of diphtheria toxin and its implications for membrane penetration. *Biochemistry* **24:**5458–5464
4. Cabiaux, V., Vandenbranden, M., Falmagne, P., Ruysschaert, J.-M. 1985. Aggregation and fusion of lipid vesicles induced by diphtheria toxin at low ph; Possible involvement of the P site and the NAD^+ binding site. *Biosci. Reports* **5:**243–250
5. Carroll, S.F., Barbieri, J.T., Collier, R.J. 1986. Dimeric form of diphtheria toxin: purification and characterization. *Biochemistry* **25:**2425–2430
6. Chattopadhyay, A., London E. 1987. Parallax Method for Direct Measurement of Membrane Penetration Depth Utilizing Fluorescence Quenching by Spin-Labeled Phospholipids. *Biochemistry* **26;**39–45
7. Chen, R.F., Knutsen, J.R. 1988. Mechanism of fluorescence concentration quenching of carboxyfluorescein in liposomes: energy transfer to nonfluorescent dimers. *Anal. Biochem.* **172:** 61–77
8. Choe, S., Bennett, M.J., Fuji, G., Curmi, P.M.G., Kantardjieff, K.A., Collier, R.J., Eisenburg, D. 1992. The crystal structure of diphtheria toxin. *Nature* **357:**216–222
9. Chung, L.A. 1988. Ph.D. Thesis
10. Chung, L.A., London, E. 1988. Interaction of diphtheria toxin with model membranes. *Biochemistry* **27:**1245–1253
11. Collier, R.J. 1982. Structure and activity of diphtheria toxin. In: *ADP-Ribosylation Reactions: Biology and Medicine.* O. Hayashi, K. Ueda, editors. pp. 573–592. Academic Press, New York
12. Defrise-Quertain, F., Cabiaux, V., Vandenbranden, M., Wattiez, R., Falmagne, P., Ruysschaert, J.-M. 1989. pH Dependent bilayer destabilization and fusion of phosphatidic large unilamellar vesicles induced by diphtheria toxin and its fragment A and fragment B. *Biochemistry* **28:**3406–3413
13. Donovan, J.J., Simon, M.I., Draper, R.K., Montal, M. 1981. Diphtheria toxin forms transmembrane channels in planar lipid bilayers. *Proc. Natl. Acad. Sci. USA* **78:**172–176
14. Falnes, P.O., Madshus, I.H., Sandvig, K., Olsnes, S. 1992. Replacement of negative by positive charges in the presumed membrane-inserted part of diphtheria toxin B fragment. Effect on mem-

brane translocation and on formation of cation channels. *J. Biol. Chem.* **267:**12284–12290
15. Gordon, V.M., Klimpel, K.R., Arora, N., Henderson, M.A., Leppla, S.M. 1995. Proteolytic activation of bacterial toxins by eukaryotic cells is performed by furin and by additional cellular proteases. *Infect. Immun.* **63:**82–87
16. Henderson, R., Baldwin, J.M., Ceska, T.A., Zemlin, F., Beckmann, E., Downing, K.H. 1990. Model for the structure of bacteriorhodopsin based on high-resolution electron cryo-microscopy. *J. Mol. Biol.* **213:**899–929
17. Hu, V.W., Holmes, R.K. 1984. Evidence for direct insertion of fragments A and B of diphtheria toxin into model membranes. *J. Biol. Chem.* **259:**12226–12233
18. Hudson, T.H., Neville, D.M., Jr. 1985. Quantal entry of diphtheria toxin to the cytosol. *J. Biol. Chem.* **260:**2675–2680
19. Hudson, T.H., Neville, D.M., Jr. 1987. Temporal separation of protein toxin translocation from processing events. *J. Biol. Chem.* **262:**16484–16494
20. Jiang, G.-S., Solow, R., Hu, V. W. 1989. Characterization of Diphtheria Toxin-induced Lesions in Liposomal Membranes. *J. Biol. Chem.* **264:**13424–13429
21. Jiang, J.X., Chung, L.A., London, E. 1991. Self-translocation of diphtheria toxin across model membranes. *J. Biol. Chem.* **266:**24003–24010
22. Kagan, B.L., Finkelstein, A., Colombini, M. 1981. Diphtheria toxin fragments forms large pores in phospholipid bilayer membranes. *Proc. Natl. Acad. Sci. USA* **78:**4950–4954
23. Lanzrein, M., Sand, O., Olsnes, S. 1996. GPI-anchored diphtheria toxin receptor allows membrane translocation of the toxin without detectable ion channel activity. *EMBO J.* **15:**725–734
24. Lanzrein, M., Falnes, P.O., Sand, O., Olsnes, S. 1997. Structure-function relatoinship of the ion channel formed by diphtheria toxin in Vero cell membranes. *J. Membrane Biol.* **156:**141–148
25. London, E. 1992. Diphtheria toxin: membrane interaction and membrane translocation. *Biochim. Biophys. Acta* **1113:**25–51
26. MacDonald, R.I. 1990. Characteristics of self-quenching of the fluorescence of lipid-conjugated rhodamine in membranes. *J. Biol. Chem.* **265:**13533–13539
27. Maliniski, J.A., Nelsestuen, G.L. 1989. Membrane permeability to macromolecules mediated by the membrane attack complex. *Biochemistry* **28:**61–70
28. McKeever, B., Sarma, R. 1982. Preliminary crystallographic investigation of the protein toxin from *Corynebacterium diphtheriae. J. Biol. Chem.* **257:**6923–6925
29. Milne, J.C., Furlong, D., Hanna, P.C., Wall, J.S., Collier, R.J. 1994. Anthrax protective antigen forms oligomers during intoxication of mammalian cells. *J. Biol. Chem.* **269:**20607–20612
30. Mindell, J.A., Silverman, J.A., Collier, R.J., Finkelstein, A. 1994. Structure-function relationships in diphtheria toxin channels: III. Residues which affect the cis pH dependence of channel conductance. *J. Membrane Biol.* **137:**45–57
31. Montecucco, C., Schiavo, G., Tomasi, M. 1985. pH-dependence of the phospholipid interaction of diphtheria-toxin fragments. *Biochem. J.* **231:**123–128
32. Papini, E., Sandona, D., Rappuoli, R., Montecucco, C. 1988. On the membrane translocation of diphtheria toxin: at low pH the toxin induces ion channels on cells. *EMBO J.* **7:**3353–3359
33. Papini E., Schiavo, G., Tomasi, M., Colombatti, M., Rappuoli, R., Montecucco, C. 1987. Lipid interaction of diphtheria toxin and mutants with altered fragment B. 2. Hydrophobic photolabelling and cell intoxication. *Eur. J. Biochem.* **169:**637–644
34. Petosa, C., Collier, R.J., Klimpel, K.R., Leppla, S.H., Liddington, R.C. 1997. Crystal structure of the anthrax toxin protective antigen. *Nature* **385:**833–838
35. Reed, J.C. 1997. Double identity for proteins of the Bcl-2 family. *Nature* **387:**773–778
36. Shiver, J.W., Donovan, J.J. 1987. Interactions of diphtheria toxin with lipid vesicles: determinants of ion-channel formation. *Biochim. Biophys. Acta* **903:**48–55
37. Silverman, J.A., Mindell, J.A., Finkelstein, A., Shen, W.H., Collier, R.J. 1994. Mutational analysis of the helical hairpin region of diphtheria toxin transmembrane domain. *J. Biol. Chem.* **269:**22524–22532
38. Sims, P.J. 1984. Complement protein C9 labeled with fluorescein isothiocyanate can be used to monitor C9 polymerization and formation of the cytolytic membrane lesion. *Biochemistry* **23:**3248–3260
39. Sims, P.J., Wiedmer, T. 1984. Kinetics of polymerization of a fluoresceinated derivative of complement protein C9 by the membrane-bound complex of complement proteins C5b-8. *Biochemistry* **23:**3260–3267
40. Song, L., Hobaugh, M.R., Shustak, C., Cheley, S., Bayley, H., Gouaux, J.E. 1996. Structure of staphylococcal alpha-hemolysin, a heptameric transmembrane pore. *Science* **274:**1859–1866
41. Wang, Y., Pablo, L,. Kachel, K., London, E. 1997. Use of Trp mutations to evaluate the conformational behavior and membrane insertion of A and B chains in whole diphtheria toxin. *Biochemistry* **36:**16300–16308
42. Wang, Y., Malenbaum, S.E., Kachel, K., Zhan, H., Collier, R.J., London, E. 1997. Identification of shallow and deep membrane-penetrating forms of diphtheria toxin T domain that are regulated by protein concentration and bilayer width. *J. Biol. Chem.* **272:**25091–25098
43. Yamaizumi, M., Mekada, E., Uchida, T., Okada, Y. 1978. One molecule of diphtheria toxin fragment A introduced into a cell can kill the cell. *Cell* **15:**245–250
44. Zalman, L.S., Wisnieski, B.J. 1984. Mechanism of insertion of diphtheri toxin: peptide entry and pore size determinations. *Proc. Natl. Acad. Sci. USA* **81:**3341–3395
45. Zhao, J.-M., London, E. 1988. Conformation and model membrane interactions of diphtheria toxin fragment A. *J. Biol. Chem.* **263:**15369–15377